

Mössbauer coherent inelastic scattering of synchrotron radiation in perfect crystals

V. A. Belyakov

Surface and Vacuum Research Centre, 117334 Moscow, Russia

(Submitted 23 December 1994)

Zh. Éksp. Teor. Fiz. **108**, 741–756 (August 1995)

A dynamical theory of coherent inelastic (accompanied by creation or absorption of phonons in the crystal lattice) Mössbauer scattering of synchrotron radiation (SR) from crystals containing nuclei of the Mössbauer isotope is developed. Two-wave dynamical diffraction theory is used to construct general equations describing inelastic Mössbauer scattering, which are analyzed for the general case and solved analytically for the cases permitting separation of polarizations. A detailed analysis of the solutions is performed for thick samples in the case of pure nuclear reflections. Some qualitatively new effects compared with the case of elastic Mössbauer scattering are revealed in inelastic Mössbauer scattering of SR. They include, for example, a larger number of frequencies in the pendelösung beats versus sample thickness, a different fine structure of the angular distribution inside the region of strong diffraction, and effectively increased transparency of samples for the resonant component in the primary and the diffraction directions. © 1995 American Institute of Physics.

1. INTRODUCTION

New perspectives have been opened by the application of modern synchrotron radiation (SR) sources to Mössbauer spectroscopy.¹ Experiments which were impossible with conventional Mössbauer sources can now be performed with modern SR sources, like experiments on inelastic (with excitation or absorption of phonons) coherent Mössbauer scattering, i.e., Mössbauer coherent scattering accompanied by phonon processes in the crystal lattice.

Unusual angular distributions in inelastic coherent Mössbauer scattering were predicted in Refs. 2 and 3. Specifically, it was shown that the direction of coherent inelastic Mössbauer scattering is practically independent of the wave vector of the phonon participating in the scattering process (the physical reason for this is the very long Mössbauer scattering time compared with the characteristic times of the crystal lattice). As a consequence of this, the angular positions of inelastic and elastic diffraction reflections practically coincide. The observable effects of such a coincidence should be present in Mössbauer experiments with conventional sources (both in scattering geometry and in absorption geometry⁴). However, the most important implications are in Mössbauer experiments with SR sources (see, for example Refs. 5–7). The problem of distinguishing the elastic and inelastic channels of Mössbauer scattering became urgent in a practical aspect. Thus, a quantitative description of these measurements requires a more exact theory than the kinematical one.^{2,3}

The present paper is devoted to the dynamical diffraction theory of inelastic coherent Mössbauer scattering in perfect crystals. General equations of inelastic coherent Mössbauer scattering are derived and analyzed. The cases of most interest for experimental investigation, involving pure nuclear diffraction maxima, are examined in detail.

2. GOVERNING EQUATIONS

In Mössbauer experiments using SR a preliminary monochromatized SR beam interacts with a sample contain-

ing nuclei of the Mössbauer isotope. One should keep in mind that the energy linewidth ΔE_s of the premonochromatized SR beam is nevertheless much wider than the Mössbauer linewidth Γ . For a typical case of Fe⁵⁷ with the Mössbauer transition energy 14.4 keV the ratio $\Delta E_s/\Gamma$ is equal 10^8 – 10^9 for an SR energy linewidth 1–0.1 eV. Therefore in a theoretical description of SR Mössbauer scattering one can assume that the SR spectral density is constant in the frequency range which is much greater than the corresponding frequencies of the hyperfine nuclear interactions and of the thermal lattice excitations in a typical situation.

That is why the processes of coherent inelastic Mössbauer scattering are present along with coherent elastic Mössbauer scattering (the dynamical theory of coherent elastic Mössbauer scattering is presented in Ref. 1, 8–10). Although the probability of an individual inelastic scattering event (with the absorption or excitation of phonons) is much lower than the probability of elastic (recoilless) scattering, the probability integrated over all phonon processes can be quite comparable with the probability of recoilless scattering. The latter is proportional to f^2 and the former to $1-f^2$, where f^2 is the Lamb–Mössbauer factor. Because nuclear resonant scattering is a slow process (compared to typical lattice times) and proceeds via two stages, the first being the absorption of a photon and the second being a transition of the nuclei to the ground state accompanied by the emission of a secondary photon, the inelastic coherent scattering involving phonons may be two different groups. In one the scattering events are, accompanied by excitation or absorption of phonons when the incident photon is absorbed by the Mössbauer nucleus, while in the other scattering is accompanied by excitation or absorption of phonons when the secondary photon is reemitted by the Mössbauer nucleus.

The most probable is inelastic scattering in which phonon absorption or excitation occurs only during absorption or reemission of a photon by the Mössbauer nucleus. This corresponds to the fact that the processes of the first group lead to a “pumping” of nonresonant quanta from the wide SR

line to the narrow Mössbauer line with linewidth Γ . But the processes of the second group lead to “pumping” of the resonant Mössbauer photons from the narrow Mössbauer line to the wide SR line. In this way the resonant and nonresonant photons are interconnected. The nonresonant photons create a current at the Mössbauer frequency and the Mössbauer quanta create a current at the frequencies in the range of the SR linewidth. This relationship may be described by two equations which follow directly from the Maxwell equations:

$$\text{curl curl } \mathbf{E}_M + \frac{\varepsilon_M}{c^2} \frac{\partial^2 \mathbf{E}_M}{\partial t^2} = \chi_{Ms}(\mathbf{r}) \mathbf{E}_s, \quad (1a)$$

$$\text{curl curl } \mathbf{E}_s + \frac{\varepsilon_s}{c^2} \frac{\partial^2 \mathbf{E}_s}{\partial t^2} = \chi_{sM}(\mathbf{r}) \mathbf{E}_M, \quad (1b)$$

where \mathbf{E}_M is the Mössbauer (resonant) component of the photon electric field, \mathbf{E}_s is the synchrotron (nonresonant) component of the electric field outside the Mössbauer linewidth, ε_M is the dielectric tensor for the resonant component of the electric field taking into account the elastic Mössbauer scattering, ε_s is the dielectric tensor for the nonresonant component (if the elastic nuclear interaction of quanta is not taken into account), and χ_{Ms} and χ_{sM} are quantities analogous to the nonlinear susceptibilities in the optics, the first of which describes generation of photons at the frequency ω_M due to the field of frequency ω_s and the second describes the generation of photons at the frequency ω_s due to emission of frequency ω_M .

The expressions for ε_M and ε_s are well known,^{1,8-10} and the expressions for $\chi_{Ms}(\mathbf{r})$ and $\chi_{sM}(\mathbf{r})$ are determined according to Refs. 2 and 3 by the amplitudes for coherent inelastic scattering, and their Fourier-transforms will be given below.

In the most general case the solution of Eqs. (1a) and (1b) is quite difficult and demands the use of numerical methods. Therefore let us outline some straightforward approximations which simplify Eqs. (1a) and (1b). One can neglect the inhomogeneous term in Eq. (1b) while describing the “pumping” of radiation into the Mössbauer line from the wide SR line because the correction to the amplitude of the SR field for each individual frequency ω_s due to the pumping from the resonant line is much less than the ratio of the corresponding linewidths $\Delta\omega_M/\Delta\omega_s$. This means that in describing the inelastic coherent Mössbauer scattering of SR the “pumping” of radiation into the Mössbauer line can be described with a high accuracy by Eq. (1a) with the assumption that the field \mathbf{E}_s in the right hand side of Eq. (1a) is determined by the interaction of the SR beam with a sample without taking into account the nuclear channel of interaction. But the contribution to \mathbf{E}_s due to the inelastic coherent Mössbauer scattering is determined in this approximation by Eq. (1b), in the right-hand side of which the amplitude \mathbf{E}_M , found, from Eq. (1a), is substituted. The corresponding contribution to the nonresonant component of radiation may be quite important in Mössbauer experiments because the intensity of this component integrated over the frequency can be comparable with the intensity of the elastic component of nuclear scattering and its angular distribution practically coincides with the angular distribution of the elastic nuclear

scattering. It can be very different from the SR angular distribution in the absence of nuclear interaction (for example, nuclear diffraction peaks can be present).

In a typical Mössbauer experiment with SR an incident SR beam also excites diffraction reflections in a sample containing Mössbauer nuclei along with the primary beam. Quite frequently a situation occurs when the diffraction reflections are due to the nuclear resonant interaction of photons and in the absence of this interaction (for photons not experiencing nuclear resonant scattering) the diffraction reflections are absent and the photons propagate in the primary beam direction only.

In most practically important cases one can use the two-wave theory of Mössbauer diffraction¹ to solve the system (1a–b). In this approximation one easily obtains (in full analogy with the case of elastic Mössbauer diffraction) the following system for the partial amplitudes of the two-wave approximation:

$$\begin{aligned} & \left(1 + \hat{\varepsilon}_M^0 - \frac{k_0^2}{\kappa^2} \right) \mathbf{E}_M(\mathbf{k}_0) + \hat{\varepsilon}_{-\tau}^M \mathbf{E}_M(\mathbf{k}_1) \\ & = \hat{\chi}_0^{Ms} \mathbf{E}_s(\mathbf{k}_0) + \hat{\chi}_{-\tau}^{Ms} \mathbf{E}_s(\mathbf{k}_1), \\ & \hat{\varepsilon}_\tau^M \mathbf{E}_M(\mathbf{k}_0) + \left(1 + \hat{\varepsilon}_M^1 - \frac{k_1^2}{\kappa^2} \right) \mathbf{E}_M(\mathbf{k}_1) \\ & = \hat{\chi}_\tau^{Ms} \mathbf{E}_s(\mathbf{k}_0) + \hat{\chi}_0^{Ms} \mathbf{E}_s(\mathbf{k}_1), \end{aligned} \quad (2a)$$

$$\begin{aligned} & \left(1 + \hat{\varepsilon}_R^0 - \frac{k_{0R}^2}{\kappa^2} \right) \mathbf{E}_s(\mathbf{k}_0) + \hat{\varepsilon}_{-\tau}^R \mathbf{E}_s(\mathbf{k}_1) \\ & = \hat{\chi}_0^{sM} \mathbf{E}_M(\mathbf{k}_0) + \hat{\chi}_{-\tau}^{sM} \mathbf{E}_M(\mathbf{k}_1), \\ & \hat{\varepsilon}_\tau^R \mathbf{E}_s(\mathbf{k}_0) + \left(1 + \hat{\varepsilon}_R^1 - \frac{k_{1R}^2}{\kappa^2} \right) \mathbf{E}_s(\mathbf{k}_1) \\ & = \hat{\chi}_\tau^{sM} \mathbf{E}_M(\mathbf{k}_0) + \hat{\chi}_0^{sM} \mathbf{E}_M(\mathbf{k}_1), \end{aligned} \quad (2b)$$

where $\mathbf{E}_M(\mathbf{k}_0)$, $\mathbf{E}_M(\mathbf{k}_1)$, $\mathbf{E}_s(\mathbf{k}_0)$, $\mathbf{E}_s(\mathbf{k}_1)$ are the partial amplitudes of the photon electric fields for the directions of the primary and diffracted beams related to the resonant and nonresonant components, respectively, as the arguments of these amplitudes are the corresponding wave vectors used, κ is the magnitude of the wave vector in vacuum, i.e. ω/c , where ω is the photon frequency and c is the light velocity, $\hat{\varepsilon}_M^0$, $\hat{\varepsilon}_\tau^M$, $\hat{\varepsilon}_R^1$, $\hat{\varepsilon}_{-\tau}^R$ are the Fourier transforms of the dielectric tensor for the resonant and nonresonant photons, $\hat{\chi}_0^{Ms}$, $\hat{\chi}_{-\tau}^{Ms}$, $\hat{\chi}_\tau^{sM}$, $\hat{\chi}_0^{sM}$ are the Fourier transforms of the quantities analogous to nonlinear susceptibilities in optics, which describe pumping of photons between the resonant and nonresonant components.

Formally, Eqs. (2a) account for both the processes of pumping of Mössbauer line, which involves lattice phonons, and the processes of recoilless SR scattering (if the quantity $\hat{\chi}_0^{Ms}$ corresponds to purely elastic scattering). However, it will be assumed below that the right-hand side of Eqs. (2a) describes only inelastic processes involving lattice phonons, because the problem of the elastic coherent Mössbauer scattering has been investigated already.^{1,8-10} Due to the linearity of Eqs. (2a) the total field of the resonant component of

radiation is a sum of the known solution of the problem of elastic coherent Mössbauer scattering and the solution of the problem of inelastic coherent Mössbauer scattering of SR considered below.

3. THE BOUNDARY-VALUE PROBLEM

For make further progress in solving the problem under consideration one should specify its geometry, i.e., specify the boundary conditions. Assume that a plane premonochromatized SR wave is incident on a perfect plane-parallel single crystal sample containing Mössbauer nuclei. Assume also that the primary beam propagation direction is identical with or close to the direction corresponding to the two-wave diffraction. In solving the problem it is naturally to use the well known parametrization for monochromatic wave diffraction,¹ where the solution is found as a function of the primary wave incidence angle and the corresponding parameter in the solution is

$$\alpha = \tau (\tau + 2\kappa) / \kappa^2, \quad (3)$$

where τ is the crystal reciprocal lattice vector and κ is the wave vector of the incident quantum out of the sample.

System (2a) for the resonant component in the SR inelastic scattering differs from the corresponding system for elastic Mössbauer diffraction by the inhomogeneous terms. With very high accuracy one can assume that the amplitudes $\mathbf{E}_s(\mathbf{k}_0)$, $\mathbf{E}_s(\mathbf{k}_1)$, entering the right part of system (2a) are determined without taking into account the SR Mössbauer scattering, i.e., they may be considered to be known. That means that the inhomogeneous terms in Eqs. (2a) are known and the solution may be presented in the form:

$$\mathcal{E} = \mathcal{E}_{in} + \sum C_p \mathcal{E}_h^p, \quad (4)$$

where the first term on the right side of Eq. (4) is a particular solution of the inhomogeneous system and the second term is a linear superposition of the general solutions of the corresponding homogeneous system. The coefficients C_p in the superposition are to be determined from the boundary conditions. Thus, the expression (4) determines the general solution for the resonant component of the field generated by the SR wave.

The field of the nonresonant component connected with inelastic coherent Mössbauer scattering is also described by an expression similar in form to Eq. (4) and may be determined in an analogous way from the solution of system (2b) if the amplitudes $\mathbf{E}_M(\mathbf{k}_0)$, $\mathbf{E}_M(\mathbf{k}_1)$ found from (4) are inserted in the right-hand sides of (2b).

We have treated the field structure in the Mössbauer scattering of SR in the case of two-wave diffraction in a general form, specifying neither the crystalline nor magnetic structure (the structure of the hyperfine fields in the Mössbauer nuclei) of a sample. Nevertheless, the general form of the solution, while is similar to Eq. (4), allows one to make some qualitative assertions about the specifics of Mössbauer scattering of SR as compared with the thoroughly studied Mössbauer diffraction of gamma-photons produced by conventional Mössbauer sources.

Let us first consider the resonant scattered component. The structure of solution (4) shows that for the scattering of SR an additional term in the resonant component emerges which is due to the creation or annihilation of the lattice phonons in the primary photon absorption stage. The resonant component of the intensity due to this term is proportional to $1-f^2$ and can be quite comparable with the intensity of the purely elastic scattering. The angular distribution of this component is the same as for the purely elastic scattering; however, the interference effects connected with the interference of the particular and general solutions of the system (2a) are present in expression (4), unlike the case of purely elastic scattering. This interference can result in intensity beats that depend on sample thickness, incidence angle, and the other parameters of the problem, as well as in the corresponding polarization beats for the scattered beam.

The angular distribution of the nonresonant scattered component connected with the creation or annihilation of lattice phonons when a photon is reemitted by the Mössbauer nucleus is almost the same as the corresponding distribution for purely elastic Mössbauer scattering. This distribution can differ substantially from the angular distribution of SR which does not experience nuclear scattering if the scattering conditions correspond to pure nuclear reflection in the Mössbauer scattering. As far as the intensity of this nonresonant component integrated over the frequency is concerned, it is proportional to $1-f^2$, i.e., can be quite comparable with the intensity of purely elastic Mössbauer scattering of SR. Just as in elastic scattering, the inelastic coherent Mössbauer scattering of SR exhibits interference between the particular and general solutions of the system (2b) in expressions like (4), which leads to beats analogous to those described for the resonant component.

In the general case the qualitative behavior of the Mössbauer scattering of SR discussed above can be quantitatively described only by numerical methods. For a quantitative illustration of these effects a specific case allowing for an essential simplification of the problem of coherent Mössbauer scattering of SR is examined in detail.

4. PURE NUCLEAR REFLECTIONS

Assume now that the SR scattering from the sample is close to the Bragg condition for purely nuclear reflection in the Mössbauer diffraction. In this limit Eqs. (2) simplify considerably because the primary SR wave is not subjected to diffraction connected to the scattering at the electrons of the sample. That is why SR wave may be considered as a plane wave propagating in the sample along the primary SR beam direction. This means that the amplitude $\mathbf{E}_s(\mathbf{k}_1)$ in (2) is equal to zero and one gets the following system:

$$\begin{aligned} \left(1 + \hat{\varepsilon}_M^0 - \frac{k_0^2}{\kappa^2}\right) \mathbf{E}_M(\mathbf{k}_0) + \hat{\varepsilon}_{-\tau}^M \mathbf{E}_M(\mathbf{k}_1) &= \hat{\chi}_0^{Ms} \mathbf{E}_s(\mathbf{k}_0), \\ \hat{\varepsilon}_\tau^M \mathbf{E}_M(\mathbf{k}_0) + \left(1 + \hat{\varepsilon}_M^1 - \frac{k_1^2}{\kappa^2}\right) \mathbf{E}_M(\mathbf{k}_1) &= \hat{\chi}_\tau^{Ms} \mathbf{E}_s(\mathbf{k}_0), \quad (5a) \\ \left(1 + \hat{\varepsilon}_R^0 - \frac{k_{OR}^2}{\kappa^2}\right) \mathbf{E}_s^M(\mathbf{k}_0) &= \hat{\chi}_0^{sM} \mathbf{E}_M(\mathbf{k}_0) + \hat{\chi}_{-\tau}^{sM} \mathbf{E}_M(\mathbf{k}_1), \end{aligned}$$

$$\left(1 + \hat{\varepsilon}_R^1 - \frac{k_{1R}^2}{\kappa^2}\right) \mathbf{E}_s^M(\mathbf{k}_1) = \hat{\chi}_\tau^{sM} \mathbf{E}_M(\mathbf{k}_0) + \hat{\chi}_0^{sM} \mathbf{E}_M(\mathbf{k}_1). \quad (5b)$$

The nonresonant components in system (5b) are marked by the indices "s" and "M" to emphasize that they originate with the inelastic scattering of the resonant component. That is why, in particular, a nonresonant component connected with inelastic scattering and propagating in the secondary (diffraction) direction arises, whose amplitude enters in the last equation of the system (5). As the amplitudes $\mathbf{E}_M(\mathbf{k}_0)$, $\mathbf{E}_M(\mathbf{k}_1)$, $\mathbf{E}_s(\mathbf{k}_0)$, $\mathbf{E}_s(\mathbf{k}_1)$ are two-component vectors, in general the systems (2) and (5) consist of eight equations for eight scalar unknown quantities and the polarizations of the partial waves in the solutions are, in general, elliptical.

Further simplifications of Eqs. (2) and (5) occur when the polarizations separate in the dynamical equations, i.e., when systems (2) and (5) decompose into two disjoint sets of equations. There are several well known cases of polarization separation¹ and it will be assumed below that one of them takes place. To be specific we shall assume below that it is the case of purely nuclear reflection in an antiferromagnet crystal when the antiferromagnet axis is in the scattering plane or perpendicular to it. In both cases the characteristic polarizations of the partial waves are linear (π - and σ -polarizations)¹ and the problem reduces to the solution of system (5a), an inhomogeneous system of two linear equations.

Resonant component of inelastic scattering

To find the resonant component in coherent inelastic SR scattering we must solve system (5a). The particular solution of (5a) has the form

$$E_M(\mathbf{k}_0) = \frac{\Delta_0}{\Delta}, \quad E_M(\mathbf{k}_1) = \frac{\Delta_1}{\Delta}, \quad (6)$$

where Δ is the determinant of system (5a), Δ_0 and Δ_1 are the determinants obtained from the matrix of system (5a) by replacing the first and second columns, respectively, with the source column. Note that the result of equating the determinant Δ to zero is the dispersion equation for the reflection under consideration in the case of purely nuclear diffraction. It is a known function of the parameter α determined by Eq. (3) (or a function of the SR wave vector projected on the surface of a sample under consideration).¹

The explicit solution of system (5a) of the form (4) for the assumed conditions may be easily written in the form

$$\begin{aligned} \mathfrak{E} = & \frac{\Delta_0}{\Delta} \exp[i(\mathbf{k}_0, \mathbf{r})] + \frac{\Delta_1}{\Delta} \exp[i(\mathbf{k}_0, \tau) \mathbf{r}] \\ & + \sum_p C_p \{ \mathbf{E}_{0p}^f \exp[i(\mathbf{k}_0^f, \mathbf{r})] + \mathbf{E}_{1p}^f \exp[i(\mathbf{k}_1^f, \mathbf{r})] \}, \end{aligned} \quad (7)$$

where the subscript "s" of the wave vectors emphasize that the values of the wave vectors relate to the case when there is no nuclear interaction of SR with the sample, the superscript "f" marks the quantities related to the eigensolutions of the elastic Mössbauer diffraction problem, and "p" labels these

solutions. In the case under consideration, of linearly polarized partial waves with the amplitudes E_{0p}^f and E_{1p}^f , the sum over p contains two terms. It must be emphasized also that, as follows from the boundary conditions, all the wave vectors entering Eq. (7) have the same tangential components. However, their normal components, generally speaking, are different and are functions of the propagation direction of the primary SR beam (parameter α).

Because the coefficients C_p in (7) are to be determined from the boundary conditions on the electric and magnetic fields, one should specify the diffraction geometry to obtain their explicit form.

For the Bragg geometry these conditions demand that the waves $\mathbf{E}_M(\mathbf{k}_0)$ and $\mathbf{E}_M(\mathbf{k}_1)$ go to zero at the front and rear surfaces of the sample which results in the following system of equations:

$$\begin{aligned} C_1 E_{01}^f + C_2 E_{02}^f + \frac{\Delta_0}{\Delta} &= 0, \\ C_1 E_{11}^f \exp[i(k_{11}^f h)] + C_2 E_{12}^f \exp[i(k_{12}^f h)] \\ &+ \frac{\Delta_1}{\Delta} \exp[i(k_{1s}^f h)] = 0, \end{aligned} \quad (8)$$

where h is the sample thickness and the superscript " \perp " marks components of the wave vectors normal to the surface.

For the Laue geometry the boundary conditions demand zero values of $E_M(\mathbf{k}_0)$ and $E_M(\mathbf{k}_1)$ at the front surface and result in the following system.

$$\begin{aligned} C_1 E_{01}^f + C_2 E_{02}^f + \frac{\Delta_0}{\Delta} &= 0, \\ C_1 E_{11}^f + C_2 E_{12}^f + \frac{\Delta_1}{\Delta} &= 0. \end{aligned} \quad (9)$$

The Bragg case for a very thick (in theory semi-infinite) sample is the easiest to solve. In this case only one eigensolution, which decays toward the sample interior, is excited in the sample and the sum in Eq. (7) reduces to one term only. Assuming that $p=1$ relates to the decaying solution one easily finds from Eq. (7):

$$E_1 = \frac{\Delta_1}{\Delta} - \frac{\Delta_0}{\Delta} \frac{E_{11}^f}{E_{01}^f}. \quad (10)$$

Expression (10) gives the amplitude of the diffracted wave as a function of the SR beam incidence angle. The right hand side of the obtained expression is a function of parameter α , depends on the SR intensity, the Lamb-Mössbauer factor, and the nuclear transition characteristics. Expression (10) describes reflection of linearly polarized SR with the polarization coinciding with the polarization of the eigensolution 1. Reflection of SR with the second linear polarization is described by a formula analogous to Eq. (10), containing the amplitudes of the second eigensolution that decay in the direction into the sample.

Nonresonant component of inelastic scattering

The field of the resonant component found above and the field of purely elastic Mössbauer diffraction determine the

nonresonant component of coherent inelastic Mössbauer scattering of SR via systems (2b) and (5b). In the case of a nuclear reflection the equations for the waves scattered in the primary and diffraction directions are uncoupled in this approximation [see Eq. (2)]. We restrict ourselves to consideration of the nonresonant component scattered in the diffraction direction only, because both the incident SR beam and the scattered SR propagate in the primary direction, and distinguishing the inelastically scattered component experimentally is more difficult than for the diffraction direction (the approach to the problem for the primary direction is completely analogous).

The scattering in the diffraction direction is described by the last equation of system (5b). As we have seen, the field of the resonant component in the sample is a linear superposition of the eigensolutions of Mössbauer elastic diffraction and the particular solutions of the inhomogeneous system (5a). That is why, in order to simplify the formulas, we assume that the inhomogeneous term in the last equation in system (5b) is determined by only one eigensolution of the elastic Mössbauer diffraction problem. From the solution found this way any other situation may be described by summing the result over all eigenmodes with appropriate weights by virtue of the linearity of the problem.

The particular solution of the last equation in system (5b) may be presented in the form

$$\mathbf{E}_s^M(\mathbf{k}_1) = \left[k_{1\parallel}^2 + k_{0\perp}^2 - \left(\frac{\omega}{c} \right)^2 \varepsilon_R \right]^{-1} [\hat{\chi}_\tau^{sM} \mathbf{E}_{0q}^f + \hat{\chi}_0^{sM} \mathbf{E}_{1q}^f], \quad (11)$$

where $k_{0\perp}^q$ is the normal component of the wave vector in the primary direction for the q th eigensolution of the elastic Mössbauer diffraction problem, $k_{1\parallel}$ is the tangential component of k_1 , and \mathbf{E}_{0q}^f and \mathbf{E}_{1q}^f are the amplitudes of the partial waves in the primary and diffraction directions (depending on the parameter α).

For the Bragg geometry the boundary condition on the desired solution reduces to the vanishing of the amplitude of the wave propagating in the diffraction direction at the exit surface and the solution takes the form

$$\begin{aligned} \mathbf{E}_s^M(\mathbf{k}_1, \mathbf{r}) = & \left[k_{1\parallel}^2 + k_{0\perp}^2 - \left(\frac{\omega}{c} \right)^2 \varepsilon_R \right]^{-1} \{ -[\hat{\chi}_\tau^{sM} \mathbf{E}_{0q}^f \\ & + \hat{\chi}_0^{sM} \mathbf{E}_{1q}^f] \exp[ih(k_{0\perp}^q - k_{1\perp})] \exp[i\mathbf{k}_1 \mathbf{r}] \\ & + \hat{\chi}_\tau^{sM} \mathbf{E}_{0q}^f \exp[i\mathbf{k}_0^q \mathbf{r}] + \hat{\chi}_0^{sM} \mathbf{E}_{1q}^f \\ & \times \exp[i(\mathbf{k}_0^q + \tau) \mathbf{r}] \}. \end{aligned} \quad (12)$$

The expression for the reflected wave amplitude following from Eq. (12) is given by the formula:

$$\begin{aligned} \mathbf{E}_s^M(\mathbf{k}_1, 0) = & \left[k_{1\parallel}^2 + k_{0\perp}^2 - \left(\frac{\omega}{c} \right)^2 \varepsilon_R \right]^{-1} \{ (\hat{\chi}_\tau^{sM} \mathbf{E}_{0q}^f \\ & + \hat{\chi}_0^{sM} \mathbf{E}_{1q}^f) (1 - \exp[ih(k_{0\perp}^q - k_{1\perp})]) \}. \end{aligned} \quad (13)$$

For a thick sample (half space) the expression (13) gives

$$\mathbf{E}_s^M(\mathbf{k}_1, 0) = \left[k_{1\parallel}^2 + k_{0\perp}^2 - \left(\frac{\omega}{c} \right)^2 \varepsilon_R \right]^{-1}$$

$$\times (\hat{\chi}_\tau^{sM} \mathbf{E}_{0q}^f + \hat{\chi}_0^{sM} \mathbf{E}_{1q}^f). \quad (14)$$

For the Laue geometry the boundary condition on the solution to be found is the vanishing of the amplitude of the wave propagating in the diffraction direction at the front surface, and the solution takes the form:

$$\begin{aligned} \mathbf{E}_s^M(\mathbf{k}_1, \mathbf{r}) = & \left[k_{1\parallel}^2 + k_{0\perp}^2 - \left(\frac{\omega}{c} \right)^2 \varepsilon_R \right]^{-1} \{ -[\hat{\chi}_\tau^{sM} \mathbf{E}_{0q}^f \\ & + \hat{\chi}_0^{sM} \mathbf{E}_{1q}^f] \exp[i\mathbf{k}_1 \mathbf{r}] + \hat{\chi}_\tau^{sM} \mathbf{E}_{0q}^f \exp[i\mathbf{k}_0^q \mathbf{r}] \\ & + \hat{\chi}_0^{sM} \mathbf{E}_{1q}^f \exp[i(\mathbf{k}_0^q + \tau) \mathbf{r}] \}. \end{aligned} \quad (15)$$

5. MÖSSBAUER SCATTERING OF SR IN THICK CRYSTALS

We illustrate the general formulas obtained above for the case of thick samples. For this we use the explicit form of the quantities $\hat{\varepsilon}_M^0$, $\hat{\varepsilon}_\tau^M$ and $\hat{\chi}_0^{Ms}$, $\hat{\chi}_\tau^{Ms}$, $\hat{\chi}_\tau^{sM}$, $\hat{\chi}_0^{sM}$ connected with nuclear interactions. These parameters of the problem depend on the unit cell structure, the existence of resonant factors is common to all of them. In the case when the Mössbauer nuclei occupy equivalent positions in the unit cell, which will be examined below, all Mössbauer nuclei have the same resonant energy, and the expressions for the parameters mentioned above are simplified. In the values $\hat{\varepsilon}_M^0$, $\hat{\varepsilon}_\tau^M$ the following resonant behavior¹ is important:

$$\begin{aligned} \Delta \hat{\varepsilon}_M^0 & \approx \frac{f^2 \Gamma_i N_0}{E_s - E_R + i\Gamma/2}, \\ \hat{\varepsilon}_\tau^M & \approx \frac{f^2 \Gamma_i N_\tau}{E_s - E_R + i\Gamma/2}, \end{aligned} \quad (16)$$

where Γ_i and Γ are the radiative width and the total width of the Mössbauer level, and N_0 and N_τ are factors depending on the unit cell structure. The analogous expressions for $\hat{\chi}_0^{Ms}$, $\hat{\chi}_\tau^{Ms}$ take the form²

$$\begin{aligned} \hat{\chi}_0^{Ms} & \approx \frac{f \sqrt{P(n_0 \rightarrow n)} \Gamma_i N_0}{E_s - E_R - [\varepsilon(n) - \varepsilon(n_0)] + i\Gamma/2}, \\ \hat{\chi}_\tau^{Ms} & \approx \frac{f \sqrt{P(n_0 \rightarrow n)} \Gamma_i N_\tau}{E_s - E_R - [\varepsilon(n) - \varepsilon(n_0)] + i\Gamma/2}, \end{aligned} \quad (17)$$

where $P(n_0 \rightarrow n)$ is the probability that the phonon state of the lattice changes a Mössbauer nucleus absorbs a photon, and $\varepsilon(n)$ and $\varepsilon(n_0)$ are the energies of the corresponding phonon states of the lattice.

Let us examine first the inelastic coherent Mössbauer scattering of the SR into the resonant component. To do this one should specify Eq. (10) with the help of Eqs. (16) and (17). The determinant Δ , in particular, can be expressed in terms of these quantities as follows (see Ref. 1):

$$\Delta = \alpha \Delta \varepsilon_M^0 - (\Delta \varepsilon_M^0 \Delta \varepsilon_M^1 - \varepsilon_\tau^M \varepsilon_\tau^M). \quad (18)$$

Finally, for the amplitude of the elastic component in the Bragg geometry one gets from Eq. (10).

$$E_1 = E_s(\mathbf{k}_0) \left\{ \chi_\tau^{Ms} \Delta \varepsilon_M^0 - \chi_0^{Ms} \varepsilon_\tau^M \right\}$$

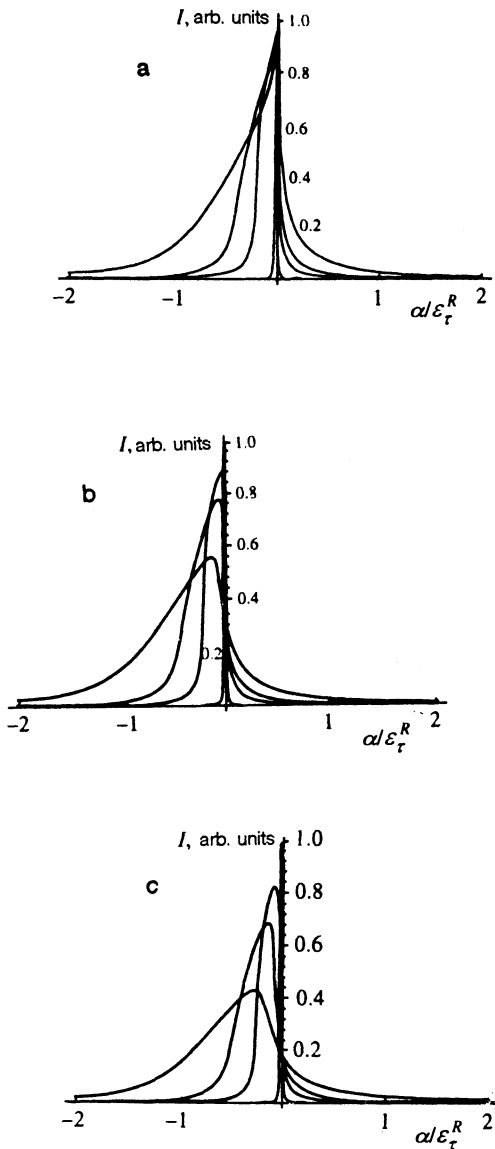


FIG. 1. The calculated angular distribution of the intensity of the resonant component in the reflected SR beam (arb. units) for a semi-infinite sample versus α/ϵ_τ^R , where ϵ_τ^R is the magnitude of ϵ_τ at exact resonance, at different departures from resonance ($\Delta E/\Gamma=1000; 100; 5; 2$) and different ratios $\text{Re}\epsilon_0/\text{Re}\epsilon_\tau$, (in (a), (b) and (c) the values of $\text{Re}\epsilon_0/\text{Re}\epsilon_\tau$ are equal to 1; 1.2; 1.4 respectively).

$$\begin{aligned}
 & -\left[\chi_0^{Ms} (\Delta\epsilon_M^1 - \alpha) - \chi_\tau^{Ms} \epsilon_\tau^M \right] \frac{E_{11}^f}{E_{01}^f} \Bigg\} \\
 & \times [\alpha \Delta\epsilon_M^0 - (\Delta\epsilon_M^0 \Delta\epsilon_M^1 - \epsilon_\tau^M \epsilon_\tau^M)]^{-1}. \quad (19)
 \end{aligned}$$

If one substitutes Eqs. (16) and (17) into Eq. (10) the expression for E_1 in the Bragg case for thick samples takes the form

$$E_1 = \frac{E_s(k_0)}{f} \sqrt{P(n_0 \rightarrow n)} \frac{E_{11}^f}{E_{01}^f}. \quad (20)$$

From Eq. (20), the angular distribution of the resonant component in inelastic coherent Mössbauer scattering of the SR from a semi-infinite sample is identical to the distribution in elastic Mössbauer scattering.

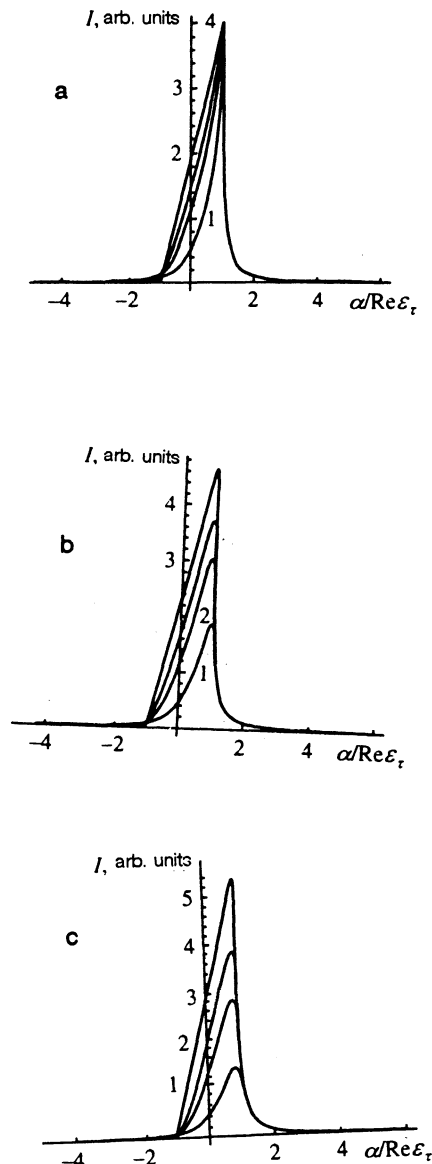


FIG. 2. The calculated angular distribution of the intensity of the nonresonant component in the reflected SR beam (arb. units) for a semi-infinite sample at different departures from the resonance in the elastic eigensolution of Mössbauer diffraction ($\Delta E/\Gamma=1000; 100; 5; 2$) and different ratios $\text{Re}\epsilon_0/\text{Re}\epsilon_\tau$, (in (a), (b) and (c) the values of $\text{Re}\epsilon_0/\text{Re}\epsilon_\tau$ are equal to 1; 1.2; 1.4 respectively).

In Fig. 1 the calculated angular distributions of the resonant component scattering for a thick sample into a pure nuclear reflection for different departures of the photon energy from the resonant energy and different ratios of the nuclear structure scattering amplitude to the corresponding forward scattering amplitude are given as functions of the deviation of the primary SR propagation direction from the Bragg direction. A typical feature of the calculated curves is a manifestation of the Kagan-Afnas'ev effect (i.e., the nuclear Borrmann effect, in which the inelastic channels of gamma-ray interaction with the nuclei are suppressed) in the form of a sharp maximum at the edge of the diffraction scattering region when the structure scattering amplitude and the corresponding forward scattering amplitude are equal. The figure also shows a sharp decrease of the angular width of

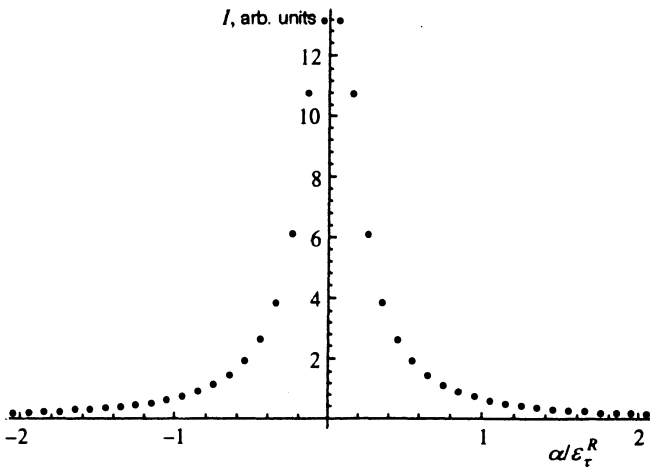


FIG. 3. The calculated angular distribution of the intensity of the resonant component in the reflected SR beam (arb. units) integrated over the energy of the incident SR beam for a semi-infinite sample versus α/ϵ_τ^R , where ϵ_τ^R is the magnitude of ϵ_τ at exact resonance, $\text{Re}\epsilon_0/\text{Re}\epsilon_\tau=1.2$. The calculated curve (see the text) corresponds to a detector acceptance angle equal to 0.05 of the angular width of the reflection curve at exact resonance).

the reflection curve as the quantum energy departs from the exact resonant value.

Moving now to the nonresonant component of the SR scattering, by substituting into Eq. (14) the explicit form of χ and ε we obtain the following expression for the denominator of Eq. (14):

$$\frac{1}{\kappa^2} \left[k_{\parallel}^2 + k_{0\perp}^2 - \left(\frac{\omega}{c} \right)^2 \varepsilon_R \right] = \frac{1}{4} \left[\alpha + \sqrt{(\alpha - 2\Delta\varepsilon_M^0)^2 - 4\varepsilon_\tau^M \varepsilon_{-\tau}^M} \right], \quad (21)$$

and the following formula for the amplitude of the inelastic component scattered in the Bragg direction:

$$E_s^M(k_1, 0) = 4 \frac{E_S \sqrt{P(n_0 \rightarrow n)} / f^2 (\varepsilon_\tau^M + \Delta\varepsilon_M^0 E_{11}^f / E_{01}^f)}{\alpha + \sqrt{(\alpha - 2\Delta\varepsilon_M^0)^2 - 4\varepsilon_\tau^M \varepsilon_{-\tau}^M}}. \quad (22)$$

Expression (22) shows (see Fig. 2) that the nonresonant component in the coherent inelastic scattering associated with scattering of an eigenmode in elastic Mössbauer diffraction differs from that of the distribution in the Mössbauer elastic scattering.

In Fig. 2 the calculated angular distributions of the resonant component of scattering from a thick sample into a pure nuclear reflection for different departures of the photon energy from the resonant energy and different ratios of the nuclear structure scattering amplitude to the corresponding forward scattering amplitude are given as functions of the deviation of the primary SR propagation direction from the Bragg direction. Note, that the curves presented in Fig. 2 (unlike the case of Fig. 1) give angular distributions of the nonresonant scattered component for a fixed photon energy as a function of the dimensionless angular variable normalized by the nuclear structure scattering amplitude dependent on the primary photon energy. This can give an impression that the angular width of the reflection curve is weakly de-

pendent on the deviation of the photon energy from the resonant value. However, the real angular widths of the reflection curves in Fig. 2, as well as in Fig. 1, are strongly dependent on the deviation from the resonance and for large deviations are inversely proportional to the deviation (the almost constant width of the reflection curves in Fig. 2 is due to the energy-dependent normalization of the angular variable).

As can be seen from Fig. 2 the calculated curves for the nonresonant scattered component are as a whole qualitatively different from the corresponding curves for the resonant component (compare with Fig. 1), decreasing more sharply as the deviation of the SR propagation direction from the Bragg direction increases. If the scattered photon energy is not detected, the observed angular distributions can be obtained with the help of the distributions presented on Figs. 1 and 2 by integration over the primary photon energies. A qualitative difference between the Mössbauer scattering of SR and scattering experiments with conventional Mössbauer sources should be noted here. This is connected with the fact that for a conventional Mössbauer source only the resonant component of the primary beam is important (spectral density of the nonresonant component is negligibly low) and usually scattering spectra that differ in the energy of the primary photon are presented. In the SR case the spectral density of the primary beam is the same both inside the resonant linewidth and out of the resonant line. Therefore in the experiments on Mössbauer scattering of SR an integration over the primary beam energy is actually performed. This sharpens the angular dependence of the scattered intensity compared with the curves given in Figs. 1 and 2.

In Fig. 3 the calculated angular distribution of SR scattering into the resonant component integrated over the primary beam energy is presented (obtained by summing curves similar to the ones presented on Fig. 1). The shape of this curve illustrates the assertion made above. The shape of the differential (in the energy) reflection curves for a semi-infinite sample (see Fig. 1) implies that the intensity of the scattered SR integrated over the initial energy should diverge if the primary beam as in the Bragg direction, because for an infinitely thick sample there is an angular range in which the reflection coefficient is finite for arbitrary large deviations of the SR energy from the resonant value. However, in the actual experiment there are always factors which limit this divergence. These are finite sample thickness, finite energy linewidth of the SR beam, and finite solid angle of the scattered radiation detection. One of these factors dominates in the actual experiment. In the calculations presented in Fig. 3 it has been assumed that a finite value of the detection solid angle is crucial for the limitation of the scattered intensity divergence (it was assumed that the corresponding angular width is equal to 0.05 of the reflection curve width for exact resonance). From the above discussion it follows also that the spectral width of the scattered SR radiation is large when the incident beam is close to the Bragg direction and the spectral width of the scattered SR radiation narrows around the resonant energy value while the incident beam direction deviates from the Bragg direction. The same can be also seen from the differential curves presented on Fig. 1. For the nonresonant component [Eq. (22)] integration over the incident

quantum energy results in a curve analogous to the curve presented on Fig. 3.

We turn now to the Laue case for the resonant component of SR inelastic scattering. As follows from the general expression (7), for an arbitrary sample beats in the intensity as a function of the sample thickness are observed with three periods [the number of possible differences between the wave vectors of the eigensolutions and the particular solution of the inhomogeneous system (5a)] in the directions of the primary and stopped waves. For the Laue case there is also a thick sample limit which differs from the case of a semi-infinite crystal. This additional limit arises because the decay rate as a function of distance into the sample is very different for the particular and the eigensolutions of the system (5). The eigensolutions decay much faster because of the nuclear interaction. That is why there is some range of sample thicknesses in which the eigensolutions are already absorbed and their interference with the particular solution is absent, but the amplitude of the particular solution is large. This is the range of sample thicknesses that corresponds to the thick sample limit for the Laue case. In the thick sample limit for the Laue case beats in the wave intensity as a function of thickness in the primary and diffraction directions disappear, and the decay rates of the resonant component intensities are described by the following formulas.

$$I_0(h) = \left| \frac{\Delta_0}{\Delta} \right|^2 \exp(-2h \operatorname{Im} k_{0s\perp}),$$

$$I_1(h) = \left| \frac{\Delta_1}{\Delta} \right|^2 \exp(-2h \operatorname{Im} k_{0s\perp}). \quad (23)$$

If the proportionality of χ and ε is taken into account, then, as in the Bragg case, one finds from Eq. (23) that the resonant component in thick crystals "survives" for the primary direction only and its intensity decays as a function of depth according to the expression

$$I_0(h) = |E_s(\mathbf{k}_0)|^2 \frac{1-f^2}{f^2} \exp(-2h \operatorname{Im} k_{0s\perp}), \quad (24)$$

where in obtaining of Eq. (24) the integration over the phonon processes has been carried out in Eq. (23). As follows

from Eq. (24), the resonant component due to the inelastic coherent scattering decays in thick crystals at the same rate as the one for the nonresonant component of SR. Thus the resonant component due to the inelastic coherent scattering becomes effectively more penetrating than the Mössbauer photons. However, this happens due to the pumping to the Mössbauer line of photons from the wide SR line.

8. CONCLUSION

This theoretical investigation of coherent inelastic Mössbauer scattering of SR in terms of the dynamical diffraction theory has revealed some qualitative new effects which cannot be described by the kinematical theory. These include the beats in beam intensities versus sample thickness, where the number of the beats differs from the case of elastic Mössbauer diffraction; the effective increase of the penetration depth of the resonant component in the beams (due to pumping of the nonresonant component into the resonant one); the details of the beam angular distributions, and so on. The estimates and computations show that many of these effects are accessible to experimental observation in existing SR sources.

¹V. A. Belyakov *Diffraction Optics of Complex Structured Periodic Media*, Moscow, Nauka, 1988, in Russian; V. A. Belyakov, *Diffraction Optics of Complex Structured Periodic Media*, Springer-Verlag, New York, 1992.

²V. A. Belyakov and Yu. M. Aivazian, *Nucl. Instrum. Methods, A* **282**, 628 (1989).

³V. A. Belyakov and Yu. M. Aivazian, *Nucl. Instrum. Methods, A* **261**, 322 (1987).

⁴V. A. Belyakov, *Hyperfine Inter.*, **67**, 633 (1991).

⁵E. Gerdau, R. Rüffer, H. Winkler *et al.*, *Phys. Rev. Lett.* **54**, 835 (1985).

⁶X. Zhang, T. Mochizuki, H. Sugiyama *et al.*, *Rev. Sci. Instrum.*, **63**, 404 (1992).

⁷Yu. Shvyd'ko, A. I. Chumakov, G. V. Smirnov *et al.*, *Europhys. Lett.*, **22**, 305 (1993).

⁸A. M. Afanas'ev and Yu. M. Kagan, *Zh. Éksp. Teor. Fiz.* **48**, 327 (1965) [*Sov. Phys. JETP* **21**, 1032 (1966)].

⁹Yu. M. Kagan, A. M. Afanas'ev and I. P. Perstnev, *Zh. Éksp. Teor. Fiz.* **54**, 1530 (1968) [*Sov. Phys. JETP* **27**, 819 (1968)].

¹⁰P. Hannon and G. T. Trammell, *Phys. Rev.* **169**, 315 (1968); *Phys. Rev.* **186**, 306 (1969).

Translated by the Author. Reproduced here with stylistic changes by the Translation Editor.